

Quantifying capability of a local seismic network in terms of locations and focal mechanism solutions of weak earthquakes

Lucia Fojtíková · Miriam Kristeková · Jiří Málek ·
Efthimios Sokos · Kristián Csicsay · Jiří Zahradník

Received: 18 April 2015 / Accepted: 24 July 2015 / Published online: 21 August 2015
© Springer Science+Business Media Dordrecht 2015

Abstract Extension of permanent seismic networks is usually governed by a number of technical, economic, logistic, and other factors. Planned upgrade of the network can be justified by theoretical assessment of the network capability in terms of reliable estimation of the key earthquake parameters (e.g., location and focal mechanisms). It could be useful not only for scientific purposes but also as a concrete proof during the process of acquisition of the funding needed for upgrade and operation of the network. Moreover, the theoretical assessment can also identify the configuration where no improvement can be achieved with additional stations, establishing a tradeoff between the improvement and additional expenses. This paper presents suggestion of a combination of suitable methods and their application to the Little Carpathians local seismic network

(Slovakia, Central Europe) monitoring epicentral zone important from the point of seismic hazard. Three configurations of the network are considered: 13 stations existing before 2011, 3 stations already added in 2011, and 7 new planned stations. Theoretical errors of the relative location are estimated by a new method, specifically developed in this paper. The resolvability of focal mechanisms determined by waveform inversion is analyzed by a recent approach based on 6D moment-tensor error ellipsoids. We consider potential seismic events situated anywhere in the studied region, thus enabling “mapping” of the expected errors. Results clearly demonstrate that the network extension remarkably decreases the errors, mainly in the planned 23-station configuration. The already made three-station extension of the network in 2011 allowed for a few real data examples. Free software made available by the authors enables similar application in any other existing or planned networks.

L. Fojtíková (✉) · J. Málek
Institute of Rock Structure and Mechanics, Academy of Sciences of the Czech Republic, v.v.i, Prague, Czech Republic
e-mail: fojtikova@irsm.cas.cz

L. Fojtíková · M. Kristeková · K. Csicsay
Earth Science Institute, Slovak Academy of Sciences, Bratislava, Slovakia

M. Kristeková
Comenius University in Bratislava, Bratislava, Slovakia

E. Sokos
Department of Geology, Seismological Laboratory, University of Patras, Patras, Greece

J. Zahradník
Faculty of Mathematics and Physics, Charles University in Prague, Prague, Czech Republic

Keywords Seismic network · Relative location uncertainty · Focal-mechanism uncertainty · Waveform inversion · Uncertainty mapping · Weak earthquakes · Little Carpathians

1 Introduction

Little Carpathians (L.C.) belong to the seismically most active zones on the territory of Slovakia. In spite currently observed weak events (Fig. 1), remarkable historical seismicity has been documented in this region. The

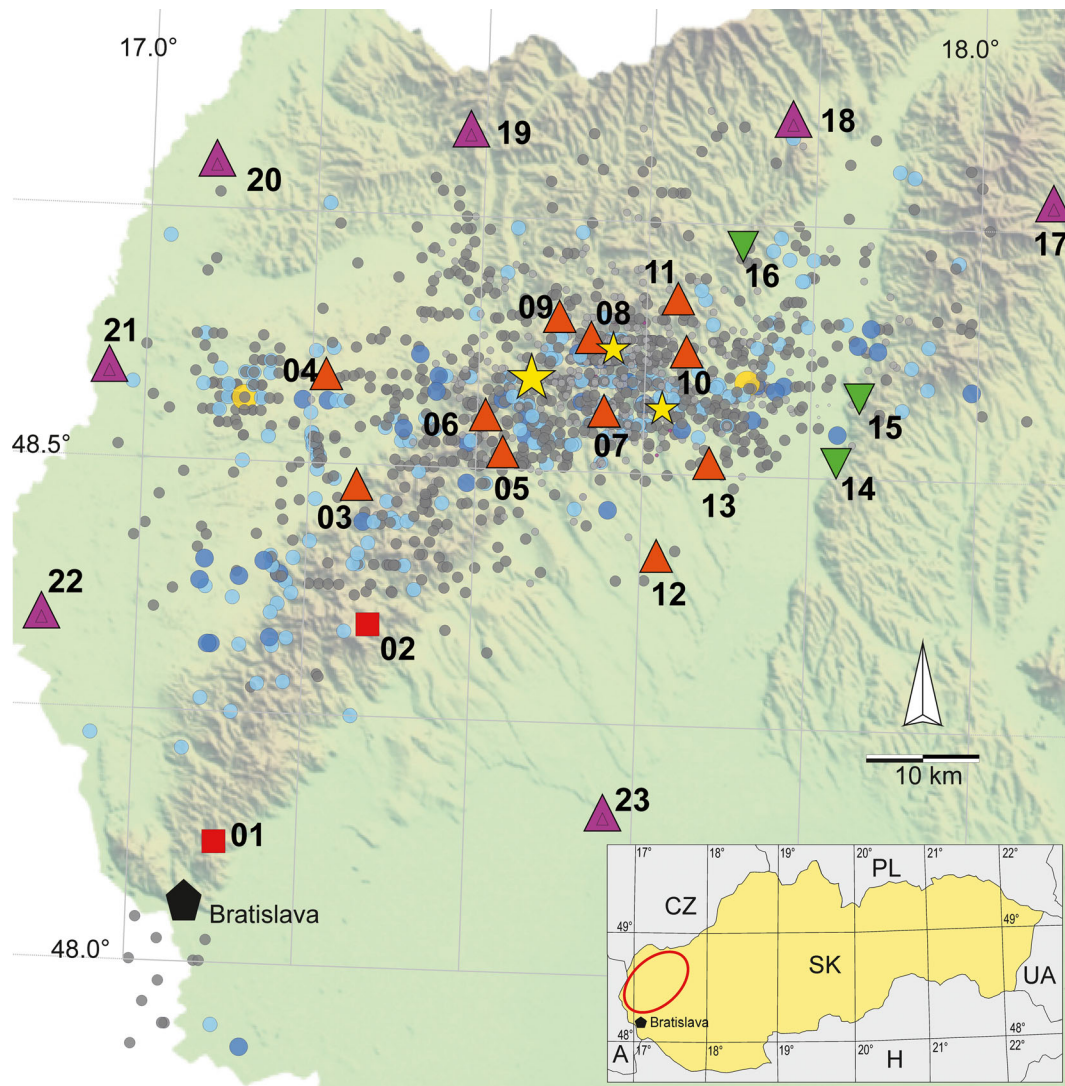


Fig. 1 The studied region, seismic stations and earthquake epicenters 3/1987–3/2013. The pre-2011 MKnet network consisted of 13 stations (*red squares and triangles*): two of them (stations ZST and MODS, nos. 1 and 2) belong to the Slovak national network of seismic stations. Three stations have been added in 2011 (nos. 14–16, *green triangles*). A further extension by seven stations (nos. 17–23, *purple triangles*) is under planning. The *yellow, blue, and gray circles* symbolize earthquakes with magnitude $M_L > 3$, $1 < M_L < 3$,

and $M_L < 1$, respectively. The historical 1906 earthquake of magnitude 5.7 is shown by *large yellow star*. The earthquakes of magnitudes > 5 , which occurred in 1906 and 1930, are shown by *small yellow stars*. *Inset* shows a broader region. The station numbers and codes: 01-ZST, 02-MODS, 03-PLAV, 04-LAKS, 05-SMO, 06-BUK, 07-KATA, 08-DVOD, 09-HRA, 10-LANC, 11-PVES, 12-SPA, 13-JABO, 14-JALS, 15-BANK, 16-PODO. Station 13 is inside the Jaslovské Bohunice power plant area

strongest documented earthquake of magnitude 5.7 occurred in the Dobrá Voda area on January 9, 1906, being followed by an event of magnitude 5.1 on January 19 (Kárník 1968; Zsíros 2005). Other earthquakes with magnitudes between 4.0 and 5.0 were observed in 1930, 1967, and 1976. Monitoring seismic activity of this source zone and careful analysis of recorded earthquakes is therefore very important for seismic hazard

assessment of the region, especially due to vicinity of nuclear power plant Jaslovské Bohunice (NPP Bohunice). In particular, exact locations and focal mechanisms improve delineation of active faults.

Little Carpathians source zone is monitored by local seismic network that has been operated by Progseis Ltd. (operation funded by NPP) since 1985. Network configuration and equipment have passed through several

significant changes from the very beginning of monitoring. The latter-day form of local L.C. seismic network has developed since 2001. Then, the sequence of the earthquakes in 2006 with strongest event $M_L=3.4$ (Lat 48.55, Lon 17.69; see Fig. 1; yellow circle in the north part of the region) outside of the network pointed out that the configuration of the local network should be extended. The three additional seismic stations at its northeastern side were built in 2011 in order to better cover the active region there (Fig. 1). These three stations have been built and are operated in cooperation of Geophysical Institute of Slovak Academy of Sciences, Institute of Rock Structure and Mechanics of the ASCR and Progseis Ltd. Most of the stations in L.C. area are equipped with 10-s sensors CMG-40T and 24-bit digitizers. The recordings are continuous with sampling frequency of 100 Hz, and data are transmitted in real time. Let us denote the virtual local network of all seismic station that are in operation in the area of interest as MKnet (MK is a shortcut from the Slovak name of Little Carpathians). The network MKnet includes also two stations of the national seismic network, MODS and ZST (operated by Geophysical Institute of Slovak Academy of Sciences), equipped with instruments STS-2 and SKD-30s, respectively.

Seismic activity of the region detected by the network MKnet in the period 3/1987–3/2013, comprised more than 1000 events of M_L from -0.5 to 3.4 (see also Fig. 1). Focal mechanisms and stress field in the region have been studied by Fojtíková et al. (2010). It can be clearly seen from Fig. 1 that there is undeniable seismic activity also outside of the current local network (including event $M_L=3.1$; yellow circle in the southwest part of the region). Therefore, seven additional not yet existing station sites have been proposed, based on several technical, logistic, and economic factors in order to further improve capabilities of the network to monitor seismic activity.

The aim of the present paper is to quantitatively evaluate usefulness of the suggested future MKnet extension, demonstrating also the improvement obtained by the already existing three-station extension (built in 2011). In other words, the problem to be solved is not to calculate the optimum position of the new stations (i.e., to make a computer design of the network), but to demonstrate and quantify improved capabilities of the extended network in terms of the key earthquake parameters (location, magnitudes, and focal mechanisms of

weak earthquakes). Influence of seismic noise should be also considered.

The location uncertainties have been studied for example by Uhrhammer (1980) and McLaren and Frohlich (1985). For example, focal mechanisms from amplitudes of very weak events and the stability of focal mechanisms have been studied for example by Stierle et al. (2014), Staňek et al. (2013), Fojtíková et al. (2010), and Šílený (2009). Focal mechanisms of weak events from waveforms have been studied for example by Šílený et al. (1996), Panza and Sarao (2000), Benetatos et al. (2013), Wéber (2009), Vavryčuk and Kuehn (2012), Zhao et al. (2014), and Fojtíková and Zahradník (2014).

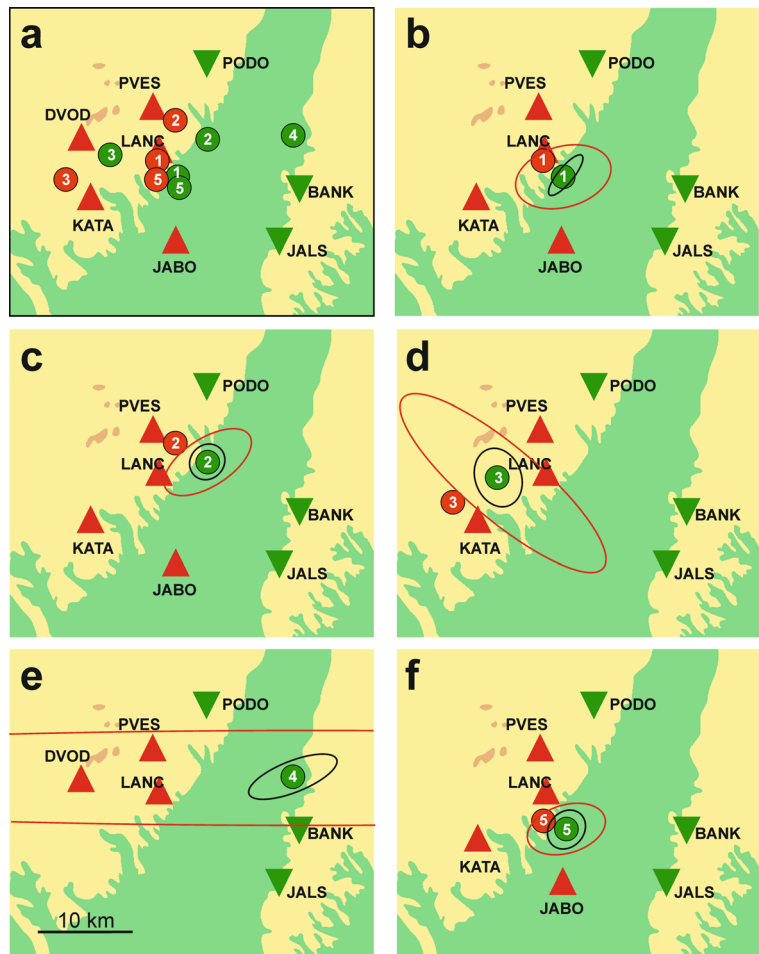
The paper is structured as follows. In Section 2, we use real data recorded after adding the three new stations in 2011 to illustrate the improvement of the location and focal mechanism determinations of weak earthquakes. In the next section, we study the intended seven-station extension of the network, assuming an arbitrary position of a seismic event within the source zone, and analyzing the corresponding uncertainties of the relative locations. To this goal, we apply a new location method developed and presented in this paper (Appendix). Finally, we map theoretical uncertainty of the moment-tensor determination using a recently developed methodology (Zahradník and Custódio 2012) which has been applied by Michele et al. (2014) to seismic network in Southern Italy.

2 Location and focal mechanism improvement—real data example

Since extension of the MKnet in 2011 by three stations (BANK Banka, JALS Jalšové, PODO Podolie), five events of $0.0 < M_L < 1.1$ have been recorded in the northeastern part of the network (Fig. 2 and Table 1). Due to the small magnitudes, the events have been located using P and S waves with stations up to epicentral distance of 15 km only. The focal mechanism has been calculated by the first-motion polarity method for event 2. In this section, we compare the locations and focal mechanisms of recorded earthquakes for the two cases—with and without the three additional stations.

Real data—location The location was made with FASTHYPO code (Herrmann 1979), using crustal velocity model of Table 2 (after Fojtíková et al. 2010). The

Fig. 2 Real data: location improvement by adding three stations in 2011. **a** Five recent events (after 2011) located without and with the three new stations BANK, JALS, and PODO are shown by *red* and *green* circles, respectively. **b–f** Error ellipsoids for events 1–5 of Table 1, calculated without and with the three new stations, are plotted in *red* and *black*. Confidence level of 68.3 % in each single parameter is considered. Note that the individual events are located with slightly different station sets, according to data availability. The event numbers, after Table 1, are shown inside the *circles*. Epicenter of event 4 located without the three new stations is out of range of **e**, and its large error ellipse (*red*) was plotted with 50 % reduction



two solutions are compared here using the pre-2011 and present-day stations. By the term pre-2011 stations, we

mean JABO, KATA, LANC, and PVES, with two exceptions: (i) for events 3 and 4, JABO station was not

Table 1 Location with the pre-2011 network (Lat 1, etc.) and with the present-day network (Lat 2, etc.)

No.	Date	Mag M_L	Lat 1 (°)	Lon 1 (°)	Depth 1 (km)	Lat 2 (°)	Lon 2 (°)	Depth 2 (km)
1	20120405 06:05:03	1.0	48.5866	17.6644	12.5	48.5716	17.6783	12.3
2	20120503 09:34:40	1.1	48.6270	17.6707	6.9	48.6095	17.7197	6.0
3	20130323 17:01:03	0.8	48.5645	17.5142	8.7	48.5905	17.5775	11.0
4	20130615 22:10:06	0.0	49.020 ^a	17.7731 ^a	0.0 ^a	48.6166	17.8450	1.1
5	20131211 22:43:57	1.0	48.5681	17.6472	6.4	48.5610	17.6814	7.8

The latter, being considered more accurate, is shown in bold; see also Fig. 2

^a Ill-posed location

Table 2 Velocity model used in this study; $V_p/V_s=1.73$

Layer top (km)	V_p (km/s)
0.0	4.00
1.9	4.80
2.5	5.60
4.5	6.00
10.0	6.20
27.0	8.20

available; (ii) for event 4, JABO and KATA were not available, and DVOD was used instead. The present-day stations include also the stations BANK, JALS, and PODO. The locations using the nearest pre-2011 and present-day stations are shown in Table 1 and Fig. 2a. Event 4 could not be located without adding the three new stations (the epicenter is falling out of the plotted area and the formal errors out of printable bounds). Except event 4, the use of three additional northeastern stations resulted in a shift of epicenters by ~ 2 –5 km, basically to east.

The two solutions are accompanied in Fig. 2b–f by their uncertainty assessment, using error ellipsoids (confidence level of 68.3 % in each single parameter marginal distribution). The error assessment has been made by standard methods based on singular vectors of linearized inverse problems (Chap. 15 of Press et al. 1997; code LOCUNC by J. Zahradník, <http://geo.mff.cuni.cz/~jz/LOCUNC/>). The ellipsoids depend only on the assumed velocity model and source station configuration. They do not depend on the real arrival time data. In practice, the ellipsoids are often plotted at the real data location epicenter, although they can be calculated for any source position. We believe that it is correct to use the same source position for both estimates, without and with the newly added stations; thus, we plot the ellipsoids into the more likely positions, those marked bold in Table 1. The uncertainty estimate in Fig. 2 is relative; it means that the ellipsoids can be compared to each other, but their absolute size (in km) remains undetermined until the arrival data and the velocity model errors are considered. Our method does not take into consideration any errors due to velocity model. To compensate for this simplification, we assume the arrival time error to be much greater than the picking error; in particular, we assumed the error of 0.3 s. Doing absolute locations and assuming data error as small as the picking error would provide nonrealistically small error ellipsoids.

We show that the network extension has a notable impact upon the improvement of the location error. For example, event 3 is located considerably better in the extended network because addition of the new station JALS improved the resolution of the epicenter position in the NW–SE direction. The most important reduction of the location error is found for event 4. The uncertainty estimate with the pre-2011 stations DVOD, LANC, and PVES is huge. The condition number (the ratio of the largest and smallest singular values) is greater than 1000. It is in agreement with complete failure of the FASTHYPO code in the real data location of event 4. When adding stations BANK, JALS, and PODO, the error is reasonable and comparable in size to other events. Similar results can be obtained for event 4 even when assuming a larger depth (e.g., 5 km).

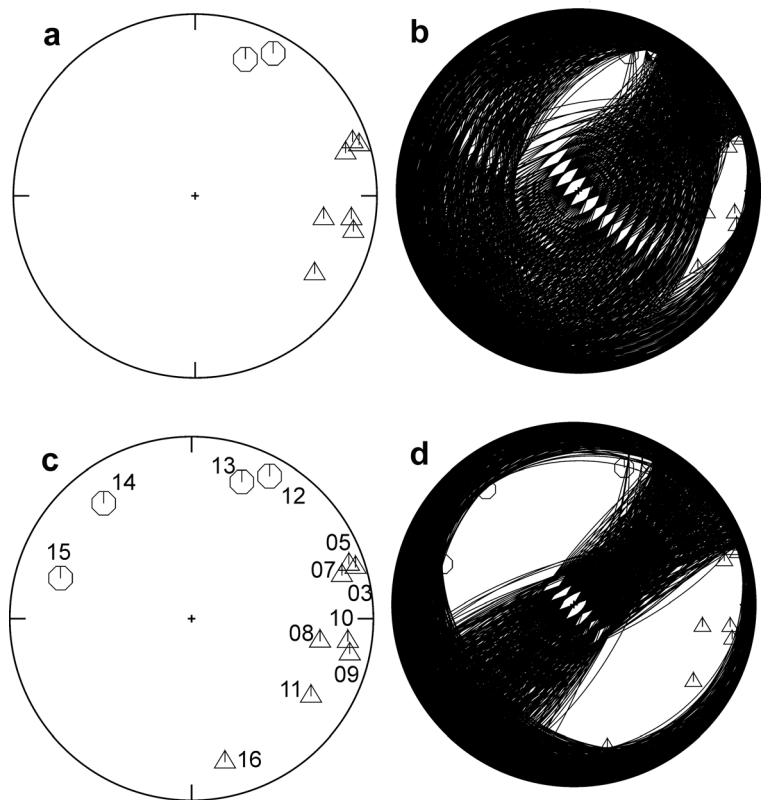
Real data—focal mechanism The result of focal mechanism analysis with FOCMEC code (Snoke 2003) based on first-motion polarities, is illustrated in Fig. 3 for event 2. Twelve first-motion polarities of the MKnet and the velocity model of Table 2 were used. Similarly to the location analysis, we applied the method twice—without and with the three new stations. To facilitate the comparison, in both cases, we assumed the same source position as the one marked bold in Table 1. As demonstrated in Fig. 3, nodal lines are considerably better clustered in the three-station extended network, hence documenting an improved resolution of the focal mechanism.

Despite currently limited availability of data (due to small magnitudes and infrequent occurrence of events during period of observation 2011–2013), these two simple examples illustrate usefulness of the three-station extension of the MKnet network in 2011. In the following section, we analyze a theoretical improvement for an arbitrary position of an event and consider influence of next extension of the network by seven planned stations.

3 Location improvement—theoretical analysis

The aim of this section is to theoretically analyze epicentral and depth errors for a source situated anywhere in a given network and thus enabling “mapping” of the expected errors. Such a problem can be simply solved by computing standard error ellipsoids (as those in the

Fig. 3 Real data: improvement of focal mechanism by adding three stations in 2011 (event 2). *Top and bottom*: the first-motion solution without and with the three stations added in 2011, respectively: **a, c** Projection of polarities (positive = circle, negative = triangle) onto lower focal hemisphere. **b, d** Nodal lines from FOCMEC code, allowing no polarity misfit. Station numbers according to Fig. 1



preceding section) for any source position in a grid covering the studied region. However, we assume that important future application will be relative location of earthquakes, because it reduces effects of limited knowledge of the velocity model in our area of interest. For the relative locations, to our best knowledge, the problem of mapping theoretical uncertainties has not been solved in literature yet. In this paper, we have developed and applied new approach enabling mapping of the expected errors of relative location for any hypocenter position using master-event location. The idea can be briefly described as follows.

Let us assume the master event located in the center of a sphere with small radius and a set of slave events situated on the sphere with regular distribution. Time differences between the theoretical onsets at couples of stations (using all combinations of stations) are calculated. Then, the same differences for slave events are calculated as well. Subtracting the differences for master and slave events (for the same couple of stations), we obtain double differences and find their maximum. Two close hypocenters can be distinguished by location procedure only in case when the double difference for a

couple of stations is bigger than the reading error (error of onset determination). Based on this criterion, an error body (of general polyhedron shape) can be constructed around the master event; while inside this error body, the master and slave event locations cannot be distinguished. More details explaining the principle of suggested method can be found in the Appendix. The program LocErr (author J. Málek) is available together with Matlab script for visualization of the results (author: M. Kristeková) at www.irsm.cas.cz/locerr.

In the present paper, only P wave onsets are considered, with an assumed picking error of 0.02 s (two samples) at all stations. The errors due to inaccurate velocity model are not considered here because they are less significant than reading errors in the relative location. Using the LocErr software, we have computed and compared location uncertainties of different station configurations for an assumed focal depth of 4 km, which is a typical depth of local earthquakes (see Fig. 4). The epicentral and depth errors are shown in the top and bottom panels of Fig. 4, respectively. Three columns represent the pre-2011 13-station network, the present-day 16-station network, and the future extension

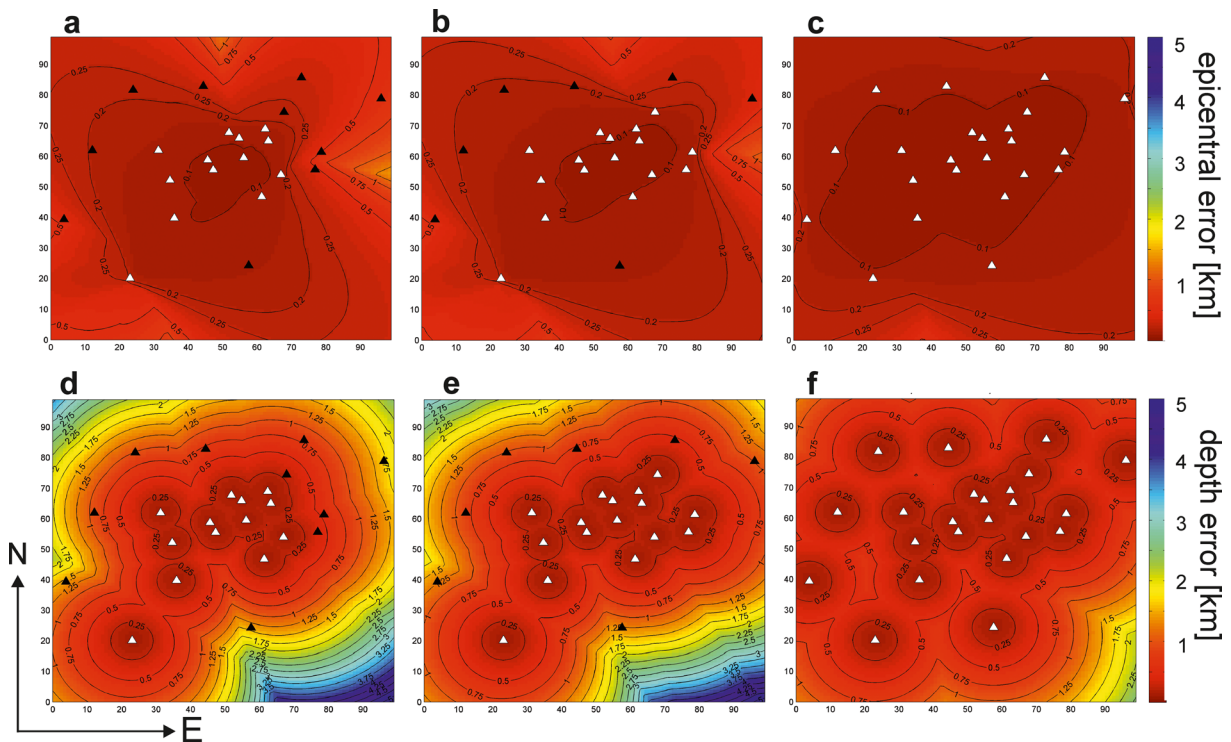


Fig. 4 Theoretical improvement of the relative location by adding three and ten stations. For a better comparison, positions of all 23 stations are shown in the figure and the used stations are shown in white: **a, d** the pre-2011 network; **b, e** the present-day network; **c, f**

the planned 23-station network. *Top and bottom* show the epicentral (i.e., horizontal) and depth errors, respectively. The plotted area is 100×100 km². The assumed source depth is 4 km. The origin (0,0) is at Lon=16.90, Lat=47.80. The axes ticks are in km

to 23 stations, respectively. The computation was performed on a 3D grid with a 1-km step covering the area 100 km×100 km×30 km. Each node of the grid is considered as a master event (see explanation of LocErr algorithm in the Appendix). The radius of sphere with slave events was set to 0.1 km. In the next, we will consider the epicentral error of ≤ 0.1 km as a tentatively chosen threshold representing good accuracy of the relative location for the studied space scale and for the assumed value of the picking error. We can see that in the case of 13 stations, the epicentral error smaller than the 0.1-km threshold is reached only in the center of the network. In case of 16 stations, this area is extended to east, but still remains relatively small. The situation improves significantly for the 23-station network of Fig. 4. As can be expected, the depth errors are larger than the epicentral errors, and we can reach the error less than 0.5 km only when the nearest station is closer than ~10 km from epicenter. Our results show that 23-station extension of the network will also enlarge this area. We have performed also computations of location uncertainties for other common depths of earthquakes in

L.C. area (9 and 14 km—not shown here), and the results also show obvious improvement for extended configurations of stations. For even deeper hypocenters (when the depth is comparable with the array aperture), the location error in depth increases with depth significantly. This effect is due to the fact that the rays between deep hypocenter and the stations are nearly parallel and the time arrivals are nearly the same at all stations at the surface.

The relative location errors could be further improved if the S wave times are included. However, in the Little Carpathians, this task is complicated by anisotropy, confirmed by the observed S wave splitting (Fig. 5.7 on p. 49 in Fojtková 2010b). Arrival time of S wave varies across the components. Therefore, we expect that in the nearest future, the relative location in this region will rely mainly on P waves.

Results of theoretical analysis using mapping of relative location errors for the three different configurations of seismic stations (pre-2011, current, and future ones) clearly demonstrate usefulness of the planned network extension.

4 Focal-mechanism improvement—theoretical analysis

Focal mechanisms in the L.C. region were calculated by Fojtíková et al. (2010) using several methods, including the waveform inversion. Small magnitudes of the post-2011 events together with current station configuration did not allow application of these approaches. However, in case of future events, it would be useful to be able to estimate moment tensors by waveform inversions; therefore, we need to evaluate their theoretical resolvability and how it can be improved by additional seismic stations. Analyzing capability of a network in terms of the focal mechanism determination is a new approach (Zahradník and Custódio 2012). The method is similar to the analysis of location uncertainties in sense that one can obtain mapping of uncertainties for a hypothetical expected earthquake source situated anywhere in a given network. Assuming a known source position and time, we relate waveform data \mathbf{d} and (six) parameters \mathbf{m} of a full moment tensor via matrix \mathbf{G} , $\mathbf{d} = \mathbf{G}\mathbf{m}$, and calculate a 6D error ellipsoid. While in the location problem, the uncertainty analysis ends with visualizing the (3D) error ellipsoid; here, we cannot visualize a 6D ellipsoid and its 2D cross sections have a limited information value. Instead, a practical approach is that we inspect the interior of the ellipsoid. To this goal, we calculate a discrete suite of points inside the ellipsoid (each one representing a focal mechanism), and we measure their deviation from a reference mechanism, corresponding to the center of the ellipsoid. In this paper, we restrict to the double-couple (DC) part of the moment tensor, because the non-DC components are in practice usually unstable. The DC part of every mechanism inside the error ellipsoid is characterized by its strike, dip, and rake. The deviation of each focal mechanism from the reference solution is quantified by Kagan's angle (Kagan 1991), hereafter denoted as K-angle. The suite of the solutions inside the error ellipsoid is characterized by a histogram of K-angle. Wherever the uncertainty has to be characterized by a single number, we choose the K-angle mean. The latter, however, has a good physical meaning only when the histogram "width" is not too large, e.g., for K-angles varying between 0° and 40° (Michele et al. 2014).

The focal mechanism uncertainty by the 6D ellipsoids has been implemented in a special tool of ISOLA software (Sokos and Zahradník 2008, 2013). The same confidence level as in the location ellipsoid is used

(68.3 % in each single-parameter). Importantly, as with any linear uncertainty analysis, this can be applied without waveform data. In terms of the relation $\mathbf{d} = \mathbf{G}\mathbf{m}$, the error ellipsoid is given by matrix \mathbf{G} , independently of \mathbf{d} and \mathbf{m} . Matrix \mathbf{G} , related to Green's functions, depends on the source station configuration, frequency range, and velocity model. In this paper, we calculate Green's functions by the discrete wavenumber method (full waveforms) and use again the velocity model of Table 2. The uncertainty analysis corresponds to mapping an assumed data error into model space. Since the data error is not well known, we assume some formal value, the so-called relative data error, and thus we estimate only a relative focal-mechanism uncertainty. Similar approach was used by Michele et al. (2014). Nevertheless, such an estimate is useful, because keeping the relative data error fixed, we are able to compare effect of changed source station configurations.

In the following examples, we assume three hypothetical events of M_w 1.6 and 2.4. This choice has been motivated by occurrence of such events in the region before extending the network. As an example, we assume a hypothetical M_w 1.6 event situated near the easternmost edge of the present-day (16-station) network. Moment tensors of weak events can be calculated by waveform inversion only in relatively short epicentral distances (Fojtíková and Zahradník 2014). A rule of thumb is that waveform modeling is possible up to distances of a few minimum shear wavelengths. For example, for shallow crustal events and frequencies approx. <1.6 Hz (wavelength ~ 2 km), it is possible to model waveforms up to ~ 10 km. High-frequency waveforms (approx. >1.6 Hz) cannot be deterministically modeled at such epicentral distances using existing velocity models because model accuracy is limited. The low-frequency limit of the inversion is given by the noise; weak events have a good signal to noise ratio only at frequencies above the microseismic noise peak (at ~ 0.2 – 0.4 Hz). Therefore, in this example, we consider the frequency range 0.8–1.6 Hz. We have selected a source position of interest and two different possible reference focal mechanisms (Fig. 5). For each one, we have performed the uncertainty analysis twice—using three near stations of the pre-2011 network, and also including the three stations built in 2011. The results, obtained without the need of real waveforms, are shown in form of nodal lines, K-angle histograms, and K-angle mean values in Fig. 5. As it is clearly demonstrated by

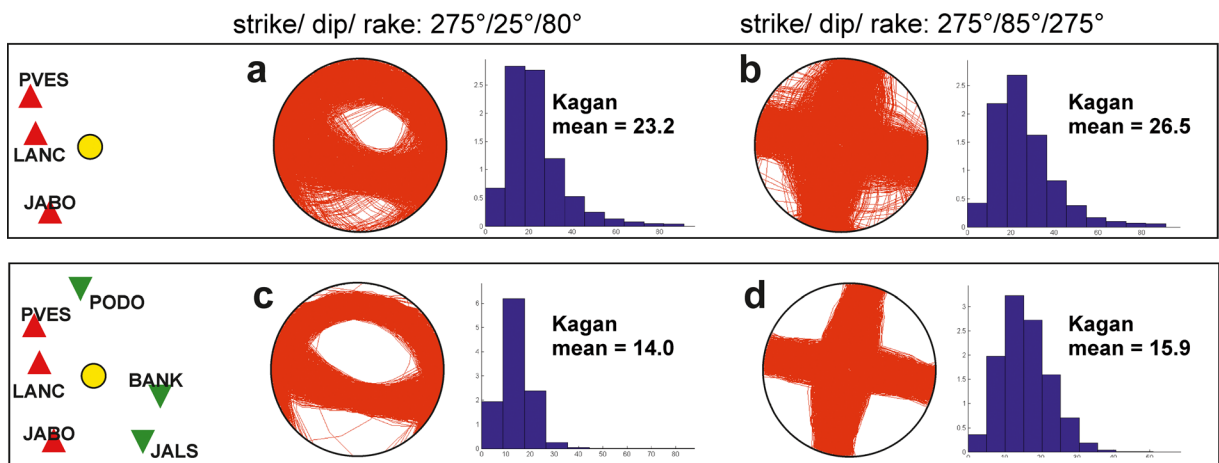


Fig. 5 Theoretical improvement of the focal mechanism by adding three stations—a single source case. The assumed source depth is 4 km. *Top*: the uncertainty analysis is applied to a selected source position (yellow circle) and three nearest stations of the pre-2011 network (red triangles). *Bottom*: adding three stations (green

triangles). Two reference focal mechanisms are considered in **a** and **c**, and **b** and **d**, respectively. The uncertainty is visualized by nodal lines, K-angle histogram, and mean values. The meaning of K-angles (degrees) is only relative, aiming at comparing efficiency of the two station configurations

the plots, addition of the three new stations has significantly reduced the focal mechanism uncertainty.

To allow mapping for an arbitrary source position, we consider a region shown in Fig. 6 covered by a 9×9 grid of trial source positions. The same uncertainty analysis (as above for a single position) is made at any point of the grid, keeping the relative data error constant. The K-angle mean value for each point is calculated and plotted in map view. An M_w 2.4 is assumed for this example. Waveform modeling for such a weak event would not be feasible in the whole MKnet due to the frequency and distance limitations discussed above. Moreover, such a weak event would be recorded with sufficient quality necessary for waveform inversion only at several near stations. Therefore, the analysis has been made separately for the N-E and N-W parts of the MKnet. Three configurations of the N-E part and two of the N-W part are analyzed in Fig. 6. The frequency inversion band suitable for the assumed event size and epicentral distances is 0.8–1.6 Hz. The reference strike/dip/rake=332°/43°/166° angles and assumed source depth 4 km have been used in this example. As was indicated by Michele et al. (2014) and also by our own results for different reference focal mechanisms (not shown here), uncertainty maps only weakly depend on the assumed mechanism. As can be seen from Fig. 6, the improvement of the MT determination by extending the network is obvious. For example, if a future event is situated in the eastern part of the network (~Lat 48.7°,

~Lon 18.2°), the K-angle improves from >30° in the pre-2011 configuration to ~20° in the present-day configuration and ~10° in the 23-station planned configuration. Similarly, the N-W extension of the network would significantly improve the moment-tensor inversions in the area.

If an expected future event is larger, e.g., M_w 4, the situation will be slightly different. Such an event would be observed with good signal to noise ratio even at longer wavelengths (i.e., lower frequencies, ~0.05–0.30 Hz); hence, we shall be able to model waveforms up to greater epicentral distances, basically for any source position within the entire MKnet. Therefore, three configurations of the network (the pre-2011, the present-day, and 23-station planned one) are compared in Fig. 7. The resolution of the focal mechanism with the network upgrade is clearly improving, not only inside the network, but, for example, also in its S-E part of the studied region where the hypothetical events have a considerable azimuthal station gap. It is a good illustration of the fact that the waveform inversion is (at least theoretically) less suffering from the azimuthal gaps than the focal mechanism determination based on peak amplitudes and polarities. Uncertainty analysis for sources situated anywhere in a region and mapping K-angles presented above have been also implemented into the broadly used and free available ISOLA software (http://geo.mff.cuni.cz/~jz/isola_2015/).

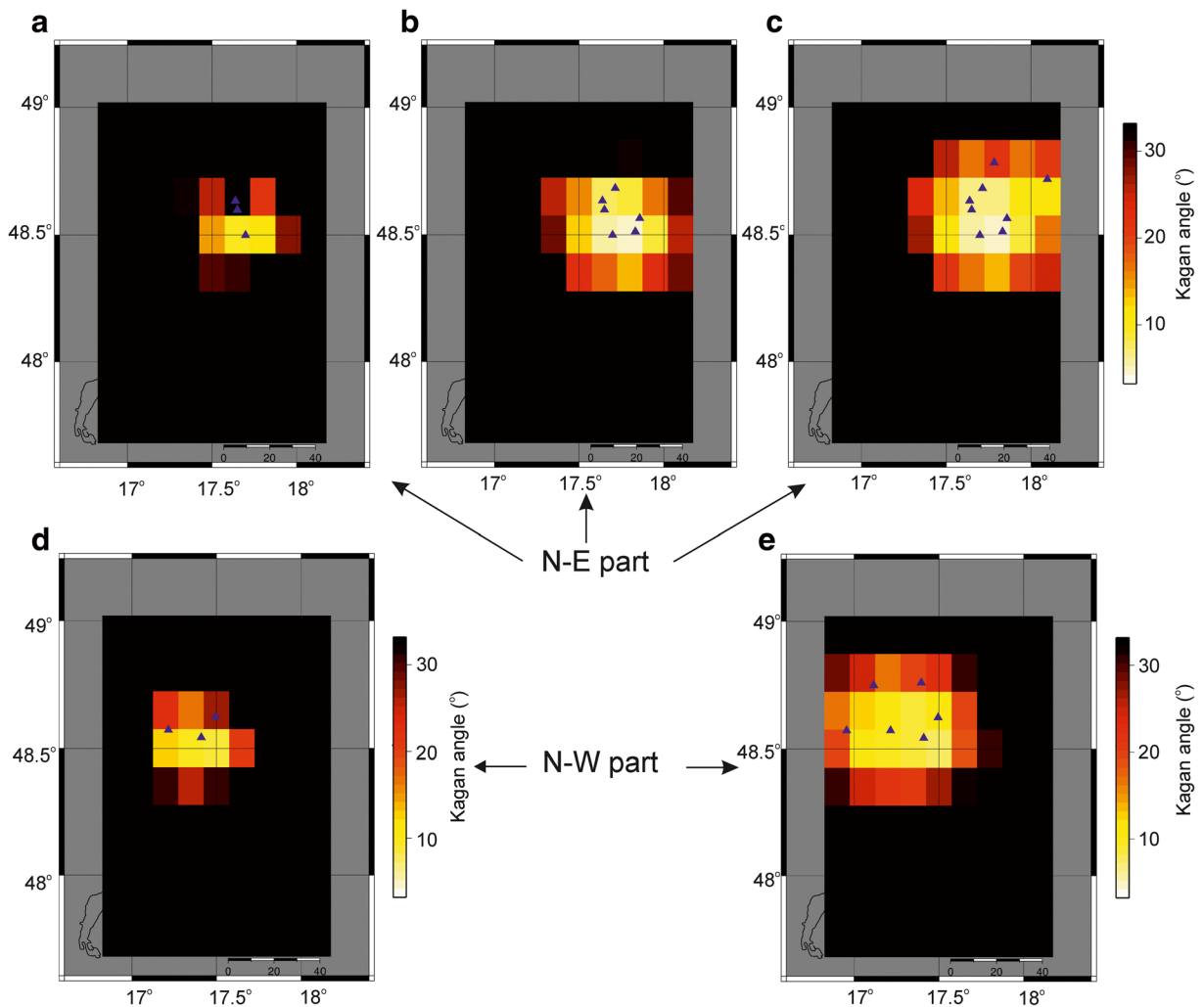


Fig. 6 Theoretical improvement of the focal mechanism by extending the network—a grid of potential sources in the N-E and N-W subregions. The uncertainty analysis is calculated for a hypothetical M_w 2.4 event situated anywhere in a 9×9 grid at a depth of 4 km. The uncertainty is mapped in terms of the K-angle mean. *Top*: the three panels correspond to the N-E part of the MKnet in its pre-2011 configuration (a), the present-day configuration (b), and the 23-station planned configuration (c), respectively. *Bottom*: the

N-W part of the network, comparing the pre-2011 (d) and the 23-station planned configuration (e) (the middle panel is missing because in the N-W subregion, the pre-2011 and present-day configurations are the same). The best moment-tensor resolution (low K-angle) is indicated by the light shade of color—white and yellow. The meaning of K-angles is only relative, aiming at comparing efficiency of various station sets

5 Conclusion

The Little Carpathians (Slovakia, Central Europe) area is an intraplate region in which weak earthquakes are presently recorded, but strong historical events have also occurred. Monitoring seismic activity of this source zone and careful analysis of recorded earthquakes is therefore important for seismic hazard assessment of

the region, especially due to immediate vicinity of nuclear power plant Jaslovské Bohunice. Seismic monitoring of the region has started in 1985 and seismic network configuration and equipment have changed several times in order to improve quality of monitoring. To name the last one, the MKnet that had consisted of 13 stations before 2011 has been upgraded by additional of 3 stations in 2011, and 7 new stations are under

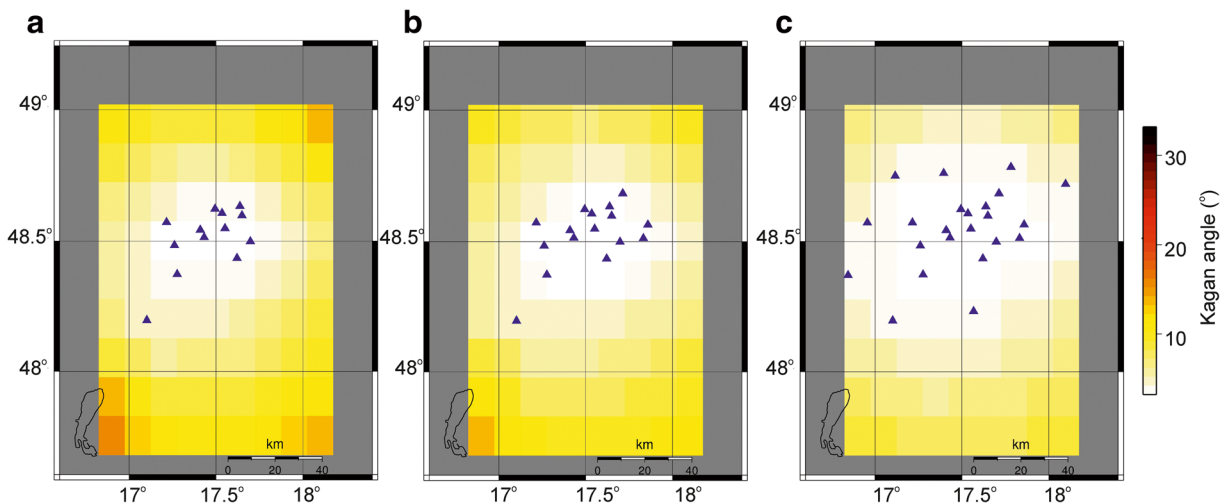


Fig. 7 Theoretical improvement of the focal mechanism by extending the network—a grid of potential sources anywhere in the entire studied region. The uncertainty analysis is calculated for a hypothetical M_w 4 event situated anywhere in a 9×9 grid at a depth of 4 km. The uncertainty is mapped in terms of the K-angle mean. **a–c** The pre-2011 configuration, the present-day configuration, and

the 23-station planned configuration of the stations, respectively. The best moment-tensor resolution (low K-angle) is indicated by the light shade of color—white and yellow. The meaning of K-angles is only relative, aiming at comparing efficiency of various configurations

consideration to better cover the assumed active region. The main purpose of this paper was to theoretically evaluate usefulness of already suggested network extension in terms of an improved earthquake location and focal mechanism determination. As a real data example, we used available data set of five weak earthquakes ($0.0 < M_L < 1.1$), recorded after 2011, showing how the three stations added in 2011 decreased the location errors. We have also demonstrated an improved resolution of the focal mechanism calculated by the first-motion polarity method for one event.

The bulk of the paper was devoted to the theoretical analysis of the network capability if earthquakes would be located by relative location methods and their moment tensors would be calculated by the full waveform inversion. Two methods were used: (i) theoretical epicentral and depth errors of the relative location were estimated by a new algorithm developed in this paper, and documented in Appendix; (ii) the moment-tensor resolvability was calculated by a recently published method (Zahradník and Custódio 2012) that was in the present paper implemented into the broadly used ISOLA code. The latter method is based on 6D moment-tensor error ellipsoids. Both

methods allow to consider seismic events situated anywhere in the studied region.

Thus, we have constructed maps of the expected location and focal mechanism errors in dependence on position of earthquake hypocenter and also for several possible types of mechanisms. The results clearly show and quantify how and where the network extension remarkably decreases the uncertainties of the location and moment tensor solutions, especially in the planned 23-station station configuration. The computer codes developed by authors have been made freely available for future applications in any other seismic network, either existing or planned. The methods presented and developed within this paper together with available computer codes provide practical tools helping to evaluate pros and cons when considering possible extension of given seismic network configuration. The network geometry, the real time data availability, and the presence of a sensitive target (the nuclear power plant) could make the network suitable, in the future, for early-warning purposes (Zollo et al. 2009)

Our results and codes, while appropriate to the Little Carpathians, have a broader application to the seismological community.

Acknowledgments Lucia Fojtíková and Jiří Málek have been supported by the Czech Science Foundation grant GACR-P210/12/2336. Jiří Zahradník has been supported by the Czech Science Foundation grant GACR-14-04372S. Miriam Kristeková, Kristian Csicsay have been supported by the Slovak Foundation Grant VEGA-2/0188/15. Miriam Kristeková has been supported as well by the project: MYGDONEMOTION APVV-0271-11, funded by the Slovak grant agency APVV. The authors thank Progseis company for providing the data from their local seismic network and Jaroslav Štrunc for cooperation in the development of new stations. The authors also thank Antonio Emolo, Ronnie Quintero, and Lucas V. Barros for constructive comments.

Appendix—LocErr method/program

A hypocenter location error is the sum of errors caused by inaccurate onset picking and simplified velocity model. In the case of relative master event location (which is implemented in LocErr), the errors caused by simplified velocity model are much smaller than in case of the absolute location. The errors are sensitive mainly to the geometrical configuration of the network under study.

The LocErr method (and also available computer program) is based on an original algorithm described below and in Fig. 8. Error bodies of a general shape (not ellipsoids) are used to characterize the so called relative double differences. They are defined as travel time differences between two stations of differences between two close hypocenters. They are normalized with expected theoretical errors.

During the location process, the origin time of earthquake is unknown (as it is the result of the location procedure). Therefore, one can measure only differences of the travel times between stations not the travel times itself. Two close hypocenters can be distinguished by a relative location procedure only in case that the double difference for a couple of stations is larger than the error of onset determination at the most sensitive pair of stations. This means that the pair of stations with minimum errors is considered here (not the average value). The computation is performed in a cubic grid of assumed master event hypocenters. For every node of the grid, the error body is computed in the following steps:

1. Travel times t_0^j are computed between the assumed master-event hypocenter and j th station of the network. Various types of velocity models can be

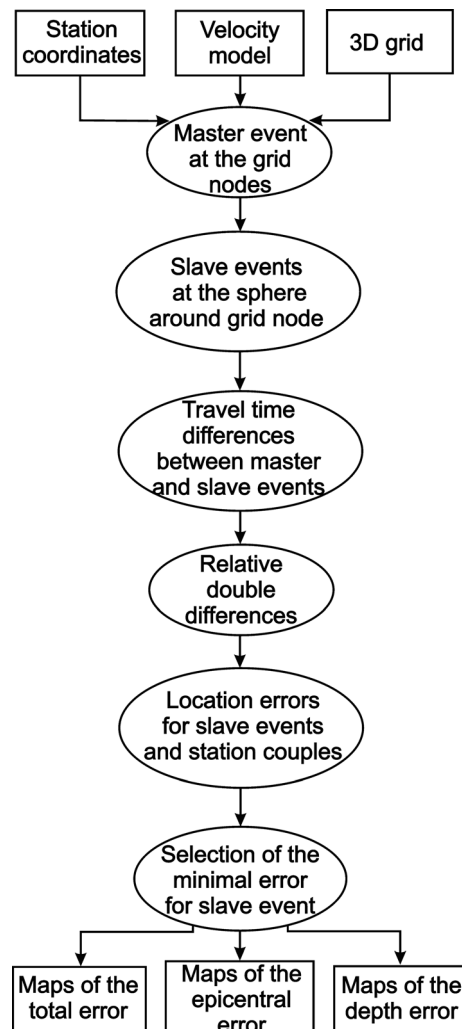


Fig. 8 The flowchart of the LocErr algorithm. Rectangles represent the inputs and output; ovals represent the procedures

used (homogeneous, layered, gradient, etc.), but the velocity model is the same for all stations and all hypocenters.

2. A sphere of a small radius around the hypocenter of master event in a grid node is defined. The choice of r_0 affects the results only slightly. The radius r_0 should be of the same order as the expected error of the location. It is important to use the same r_0 for all grid nodes, as we want to compare location errors in the whole area of seismic network.
3. A set of regularly distributed vectors and corresponding points on the sphere is defined. These points represent hypocenters of virtual slave

events. The travel times t_i^j for i th slave event and j th station are computed.

4. Travel time differences $dt_i^j = t_i^j - t_0^j$ between the master and slave events on the sphere are computed for all stations.
5. Relative double differences are computed for all combinations of stations ($j \neq k$).

$$Dt_i^{jk} = \frac{dt_i^j - dt_i^k}{\sigma^j + \sigma^k}, \quad (1)$$

where σ^j is the time picking error at j th station.

The picking errors σ are in general different for the P and S waves and can depend also on other factors such as epicentral distance, magnitude, or noise.

6. Estimate of the location error ε_i^{jk} in the direction of i th slave event corresponding to the double differences from j th and k th stations is

$$\varepsilon_i^{jk} = r_0 / Dt_i^{jk}, \quad j \neq k \quad (2)$$

7. For every slave event, the combination of stations that gives the minimum location error E_i , is found

$$E_i = \min^{jk} \left(\varepsilon_i^{jk} \right), \quad j \neq k \quad (3)$$

This expression defines an error body around the grid node. The shape of the error body is a general polyhedron.

8. The maximum error on the error body is “total error,” E_T .
9. Projection of the error body to the horizontal plane is computed, and the maximum error in this projection corresponds to an “epicentral error,” E_E .
10. Similarly, projection of the error body to the vertical axis is computed and the maximum error in this projection corresponds to “depth error,” E_D .

References

- Benetatos C, Málek J, Verga F (2013) Moment tensor inversion for two micro-earthquakes occurring inside the Hájce gas storage facilities, Czech Republic. *J Seismol* 17:557–577. doi:10.1007/s10950-012-9337-0
- Fojtíková L (2010b) Earthquake moment tensors and tectonic stress in Malé Karpaty Doctoral thesis (*in Slovak*) http://www.fyzikazeme.sk/mainpage/prace/2010_PhD_Fojtikova.pdf
- Fojtíková L, Zahradník J (2014) A new strategy for weak events in sparse networks: the first-motion polarity solutions constrained by single-station waveform inversion. *Seismol Res Lett* 85:1265–1274. doi:10.1785/0220140072
- Fojtíková L, Vavryčuk V, Čipciar A, Madarás J (2010) Focal mechanisms of micro-earthquakes in the Dobrá Voda seismoactive area in the Malé Karpaty Mts. (Little Carpathians), Slovakia. *Tectonophysics* 492:213–229
- Herrmann RB (1979) FASTHYPO—a hypocenter location program. *Earthq Notes* 50(2):25–37
- Kagan YY (1991) 3-D rotation of double-couple earthquake sources. *Geophys J Int* 106:709–716. doi:10.1111/j.1365-246X.1991.tb06343.x
- Kárník V (1968) Seismicity of the European Area. Part 1. Academia, Praha
- McLaren JP, Fröhlich C (1985) Model calculations of regional network locations for earthquakes in subduction zones. *Bull Seismol Soc Am* 75:397–413
- Michele M, Custódio S, Emolo A (2014) Moment tensor resolution: case study of the Irpinia seismic network, Southern Italy. *Bull Seismol Soc Am* 104:1348–1357. doi:10.1785/0120130177
- Panza GF, Sarao A (2000) Monitoring volcanic and geothermal areas by full seismic moment tensor inversion: are non-double-couple components always artefacts of modelling? *Geophys J Int* 143:353–364
- Press WH, Teukolsky SA, Vetterling WT, Flannery BP (1997) *Numerical Recipes in Fortran 77: The Art of Scientific Computing*, Second Ed., Cambridge University Press, 992 pages.
- Šílený J (2009) Resolution of non-double-couple mechanisms: Simulation of hypocenter mislocation and velocity structure mismodeling. *Bull Seismol Soc Am* 99(4):2265–2272. doi:10.1785/0120080335
- Šílený J, Campus P, Panza GF (1996) Seismic moment tensor resolution by waveform inversion of a few local noisy records - I. Synthetic tests. *Geophys J Int* 126:605–619
- Snoke JA (2003) FOCMEC: FOCal MECHANISM determinations. In: Lee WHK, Kanamori H, Jennings PC, Kisslinger C (eds) *International handbook of earthquake and engineering seismology*. Academic Press, San Diego, Chapter 85.12
- Sokos E, Zahradník J (2008) ISOLA a Fortran code and a Matlab GUI to perform multiple-point source inversion of seismic data. *Comput Geosci* 34:967–977
- Sokos E, Zahradník J (2013) Evaluating centroid-moment-tensor uncertainty in the new version of ISOLA software. *Seismol Res Lett* 84:656–665
- Staňek F, Eisner L, Moser TJ (2013) Stability of source mechanisms inverted from P-wave amplitude microseismic monitoring data acquired at the surface. *Geophys Prospect* 62:475–490. doi:10.1111/1365-2478.12107
- Stierle E, Vavryčuk V, Šílený J, Bohnhoff M (2014) Resolution of non-double-couple components in the seismic moment tensor using regional networks—I: a synthetic case study. *Geophys J Int* 196:1869–1877. doi:10.1093/gji/ggt502
- Uhrhammer RA (1980) Analysis of small seismographic station networks. *Bull Seismol Soc Am* 70:1369–1379
- Vavryčuk V, Kuehn D (2012) Moment tensor inversion of waveforms: a two-step time-frequency approach. *Geophys J Int* 190:1761–1776. doi:10.1111/j.1365-246X.2012.05592.x

- Wéber Z (2009) Estimating source time function and moment tensor from moment tensor rate functions by constrained L1 norm minimization. *Geophys J Int* 178:889–900
- Zahradník J, Custódio S (2012) Moment tensor resolvability: application to southwest Iberia. *Bull Seismol Soc Am* 102:1235–1254. doi:[10.1785/0120110216](https://doi.org/10.1785/0120110216)
- Zhao P, Oye V, Kuhn D, Cesca S (2014) Evidence for tensile faulting deduced from 614 full waveform moment tensor inversion during the stimulation in the Basel enhanced 615 geothermal system. *Geothermics* 52:74–83. doi:[10.1016/j.geothermics.2014.01.003](https://doi.org/10.1016/j.geothermics.2014.01.003)
- Zollo A, Iannaccone G, Lancieri M, Cantore L, Convertito V, Emolo A, Festa G, Gallovič F, Vassallo M, Martino C, Satriano C, Gasparini P (2009) The earthquake early warning system in Southern Italy: methodologies and performance evaluation. *Geophys Res Lett* 36:L00B07. doi:[10.1029/2008GL036689](https://doi.org/10.1029/2008GL036689)
- Zsíros T (2005) Seismicity of the Western-Carpathians. *Acta Geod Geophys Hung* 40:1217–8977